Linear and nonlinear analysis of normal and CAD-affected heart rate signals

ACHARYA, U Rajendra, FAUST, Oliver <http://orcid.org/0000-0002-0352-6716>, SREE, Vinitha, SWAPNA, G, MARTIS, Roshan Joy, KADRI, Nahrizul Adib and SURI, Jasjit S

Published version

ACHARYA, U Rajendra, FAUST, Oliver, SREE, Vinitha, SWAPNA, G, MARTIS, Roshan Joy, KADRI, Nahrizul Adib and SURI, Jasjit S (2014). Linear and nonlinear analysis of normal and CAD-affected heart rate signals. Computer methods and programs in biomedicine, 113 (1), 55-68.

Linear and Nonlinear Analysis of Normal and CAD-affected Heart Rate Signals

U Rajendra Acharya[a,b], Oliver Faust[a,d], Vinitha Sree[c], Swapna G[f], Roshan Joy Martis[a], Nahrizul Adib Kadri[b], Jasjit S Suri[g]

[a]*Department of Electronics and Communication Engineering, Ngee Ann Polytechnic, Singapore 599489*

[b]*Department of Biomedical Engineering, Faculty of Engineering, University of Malaya, 50603 Kuala Lumpur, Malaysia*

[c]*Global Biomedical Technologies Inc., CA, USA*

[d]*School of Electronic Information Engineering, Tianjing University, China*

[e]*School of Electrical Engineering, University of Aberdeen, Aberdeen*

[f]*Department of Applied Electronics & Instrumentation, Government Engineering College, Kozhikode, Kerala 673005, India*

[g]*Fellow AIMBE, CTO, Global Biomedical Technologies, CA, USA; Biomedical Engineering Department, Idaho State University (Aff.), ID, USA*

*Corresponding author: Oliver Faust, email: faust_o@web.de

Abstract

Coronary Artery Disease (CAD) is one of the dangerous cardiac disease, often may lead to sudden cardiac death. It is difficult to diagnose CAD by manual inspection of electrocardiogram (ECG) signals. To automate this detection task, in this study, we extracted the Heart Rate (HR) from the ECG signals and used them as base signal for further analysis. We then analyzed the HR signals of both normal and CAD subjects using (i) time domain, (ii) frequency domain and (iii) nonlinear techniques. The following are the nonlinear methods that were used in this work: Poincare plots, Recurrence Quantification Analysis

(RQA) parameters, Shannon entropy, Approximate Entropy (ApEn), Sample Entropy (SampEn), Higher Order Spectra (HOS) methods, Detrended Fluctuation Analysis (DFA), Empirical Mode Decomposition (EMD), Cumulants, and Correlation Dimension. As a result of the analysis, we present unique recurrence, Poincare and HOS plots for normal and CAD subjects. We have also observed significant variations in the range of these features with respect to normal and CAD classes, and have presented the same in this paper. We found that the RQA parameters were higher for CAD subjects indicating more rhythm. Since the activity of CAD subjects is less, similar signal patterns repeat more frequently compared to the normal subjects. The entropy based parameters, ApEn and SampEn, are lower for CAD subjects indicating lower entropy (less activity due to impairment) for CAD. Almost all HOS parameters showed higher values for the CAD group, indicating the presence of higher frequency content in the CAD signals. Thus, our study provides a deep insight into how such nonlinear features could be exploited to effectively and reliably detect the presence of CAD.

***Keywords*:** heart rate, CAD, ECG, HOS, Poincare plot, recurrence plot, EMD.

1. Introduction

Coronary arteries supply nutrients and oxygen to heart muscles. Coronary Artery Disease (CAD) is a pathological condition where the diameter of the arteries decreases either due to the formation of cholesterol plaque on its inner wall [Steinberget al., 1999] or due to the contraction of the whole wall for other reasons, such as tobacco smoking [Ockene et al., 1997] and environmental pollution [Brook et al., 2004]. The condition is often ominously silent, but progressive in nature. If it is not treated appropriately, it will eventually lead to ischemia (i.e., interruptions of blood supply) and then infarctions (i.e., the complete loss of blood supply). Usually one of the reasons for Sudden Cardiac Death (SCD) is CAD [Thompson et al., 2006]. Hence, early detection of CAD is essential to prevent SCD.

One of the most commonly used techniques for CAD detection is the Exercise Stress Test (EST). EST increases the workload of the heart and records exaggerated electrophysiological information. For this test to be accurate, a target Heart Rate (HR) has to be attained. Not all CAD patients can reach this rate. Furthermore there is considerable risk

for the patient, because such a stress test can trigger Ventricular Tachycardia (VT) or cardiac arrest [San Roman et al., 1998].

Electrocardiogram (ECG) could be a useful physiological measurement tool to detect the presence of CAD. However, visual interpretation of the ECG signals is not so effective as 50 - 70% of CAD patients do not show any notable difference in their ECGs [Silber et al., 1975]. However, the minute variations in the ECG signals have to identified in order to diagnose specific type of heart disease. Due to the presence of noise and baseline wander, it is tedious to detect the minute variations by evaluating the morphological features of ECG signals. Hence, in this study, we extracted the HR from the ECG signals and used them for analysis. The study of Heart Rate Variability (HRV) is a better technique to diagnose CAD risk levels. HR is a nonlinear, non-stationary signal which indicates the subtle variations of the underlying ECG signal [Acharya et al., 2004a]. The HRV evaluates the changes in the consecutive heart rates and it assesses the health of the Autonomic Nervous System (ANS) non-invasively. The HRV analysis conveys information about homeostasis of the body [Lombardi 2000]. Standard methods to analyze the HRV were proposed in various domains [Task Force, 1996].

Various cardiac and non-cardiac diseases have been diagnosed using HR signals[Isler et al., 2007, Schumann et al., 2002, Acharya et al., 2004a, Gujjar et al., 2004, Carney et al., 2000]. They have analyzed the HR signals using various linear and non-linear techniques [Acharya et al., 2004a; 2007]. Huikuri et al. (1994) have analyzed the CAD subjects using HRV signals and showed that, the circadian rhythm decreases in CAD subjects. Hayano et al. (1990) have shown a correlation between CAD severity and a reduction low-frequency power . reduction decrease in high frequency power were shown in CAD subjects [Lavoie et al. (2004), Nikolopoulos et al. (2003)] and features of time and frequency domain were found to be lower for CAD subjects[Bigger et al. (1995)]. The statistical measures changes with time and hence time domain analysis is not effective and effectiveness of frequency domain analysis decreases with reduction in the signal to noise ratio [Acharya et al., 2006].

Nonlinear techniques are more in tune with the nature of physiological signals and systems, therefore, they outperform time and frequency domain methods. Hence, they are widely used in many biological and medical applications [Acharya et al., 2003; Fell et al.,

2000]. Owis et al. (2002) performed ECG-based arrhythmia detection and classification based on nonlinear modeling. Sun et al. (2000), Acharya et al. (2007) and Chua et al. (2008) used nonlinear techniques to analyze cardiac signals for the development of cardiac arrhythmia detection algorithms. Schumacher et al. (2004) elaborated the effectiveness of linear and nonlinear techniques in analyzing HR signals. The onset of various cardiovascular diseases like, Ventricular Tachycardia (VT) and Congestive Cardiac Failure (CCF) can be predicted using non-linear analysis of HR signals [Cohen et al. 1996]. Chua et al. (2006) introduced a method to extract features like bispectral entropy from HR signals by employing Higher Order Spectra (HOS) techniques. In their study, HOS features from HR signals were used to differentiate between a normal heart beat and seven arrhythmia classes. CAD results in reduced Baroreflex Sensitivity (BRS) and reduced vagal activity which can be understood by HRV analysis. BRS is an indicator of increased risk of SCD in myocardial infarction patients. Arica et al. (2010) used HR and systolic pressure signals to assess BRS.

The main aim of this paper is to present time, frequency and non-linear features for normal and CAD-affected HR signals. For this analysis, we extracted and analyzed features in the time domain, frequency domain, and also studied features derived using nonlinear methods. Furthermore, we have proposed various ranges for these features and presented unique nonlinear plots for the normal and CAD classes. Our results show that CAD subjects have less variability in their heart rate signal when compared to normal subjects. This reduced variability can be used as a single measure to diagnose CAD from ECG signals which were obtained under normal conditions. We predict that the consequent use of HRV measures will reduce the need to conduct stress ECG measurements, and therefore, expose patients to less risk.

2. Data Used

ECG signals from 10 CAD patients and an equal number of healthy volunteers were recorded using the BIOPAC™ equipment [http://www.biopac.com/]. The sampling frequency of ECG signal was 500 Hz. The average age of both normal and CAD subjects was 55 years (age varied from 40 to 70 years). The CAD patients used for this study, were taken from Iqraa Hospital, Calicut, Kerala, India. Subjects having normal blood pressure,

glucose level and ECG were considered in the *normal* category. For the *CAD* patients, coronary angiography (CAG) was performed. Patients with more than 50% narrowing in the left main artery were considered for this study. Patients suffering from bundle branch block (left or right bundle branch block), hypertrophy, atrial fibrillation, congestive heart failure, myopathy, and taking any cardiac medication are excluded in this study. The patients were selected by a cardiologist based on the similarity of their medications. It was assumed that the drug effects on the HR signal were similar. The data comprised a total of 61 normal and 82 ECG CAD datasets; each set had 1000 samples from 10 subjects. The variations of ECG signals in CAD and normal subjects are shown in Figure 1.

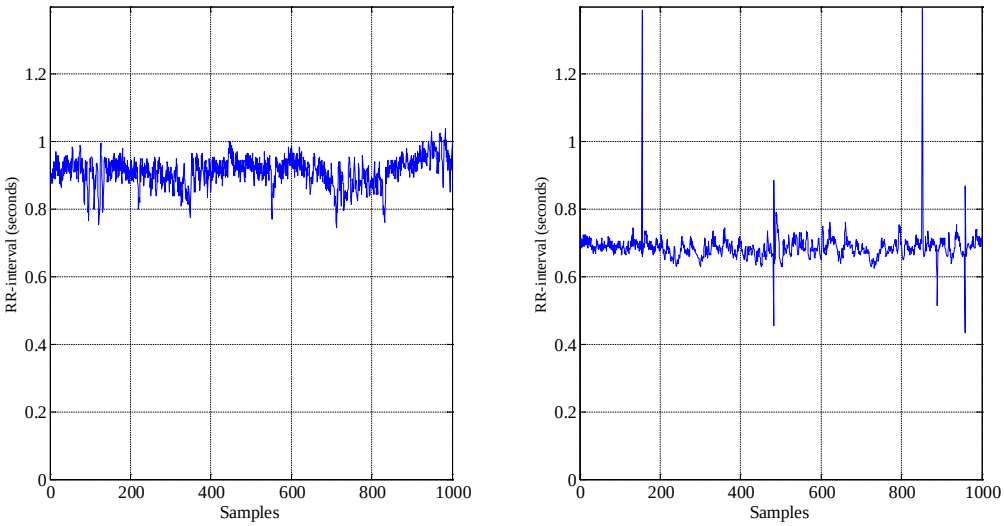

(a) (b)

Figure 1 Typical RR signal: (a) normal (b) CAD.

The ECG beats were sent via a band pass filter with a lower cut off frequency of 0.3 Hz to eliminate baseline wander and higher cut off frequency of 50 Hz to eliminate the noise. A band-stop flter of cut-off frequency 50 Hz was used to eliminate power source influences. In the final step, the *R* peaks were located using Pan and Tompkins algorithm [Pan et al., 1985, Wariar et al., 1991]. The time duration between two consecutive R peaks is termed as RR interval (t_{RR}). Heart rate is defined as:

$$HR_{bpm} = \frac{60}{t_{RR}} \quad \text{(Beats Per Minute)} \tag{1}$$

3. Methods Used

This section discusses time, frequency and nonlinear domain techniques which were used for analyzing CAD and normal HR signals.

3.1. Time domain analysis

RR interval is one of the time domain parameter which reflects the combined influence of SNS and PNS. The mean of the RR time intervals is the mean RR parameter. Most of the time domain parameters (both short term and long-term variation indices) are derived from the RR intervals. Apart from the RR interval, we have calculated RMSSD (root mean square standard deviation), NN50 (number of pairs of consecutive NNs which vary greater than 50 ms) and pNN50 (ratio of NN50 divided by total number of NNs). RMSSD (in milliseconds) indicates the parasympathetic control of HR during the normal rhythm.

3.2. Frequency domain analysis

The above discussed time domain technique is easy to implement and use. But its ability to separate sympathetic and parasympathetic influences using heart rate signal is limited. The cardiac health of the subject can be evaluated using the power spectrum of the HR signal [Akselrod et al., 1981]. There are the three main frequency regions of the heart rate signal.

- The power in the frequency range from 0.15 Hz to 0.5 Hz is defined as high frequency (HF) power band.
- The power in the frequency range from 0.0.4Hz to 0.15 Hz is defined as low frequency (LF) power band.
- The power in the frequency range from 0.0033Hz to 0.04 Hz is defined as very-low-frequency (VLF) power band.

HF region is an indicator of the vagal activity and respiratory sinus arrhythmia (RSA), while LF refers to the baroreceptor control mechanisms and the combined effect of sympathetic and vagal systems. The VLF power spectrum indicates the vascular mechanisms and rennin-angiotension systems. In our work, we measured total power, HF, LF as well as the ratio of LF to HF power.

Frequency domain study is normally conducted using by using the using Fast Fourier Transform to estimate the Power Spectral Density (PSD) . AR (Autoregressive) modeling is also a frequency domain analysis method [Faust et al., 2004]. The AR parameters are estimated by solving linear equations. A suitable filter order has to be selected. . In this study, we have used order of AR model as 16 [Akaike, 1969; 1974; Anita et al., 2002]. Figure 2 shows the typical PSD of a normal HR signal (Figure 2(a)) and a CAD HR signal (Figure 2(b)).

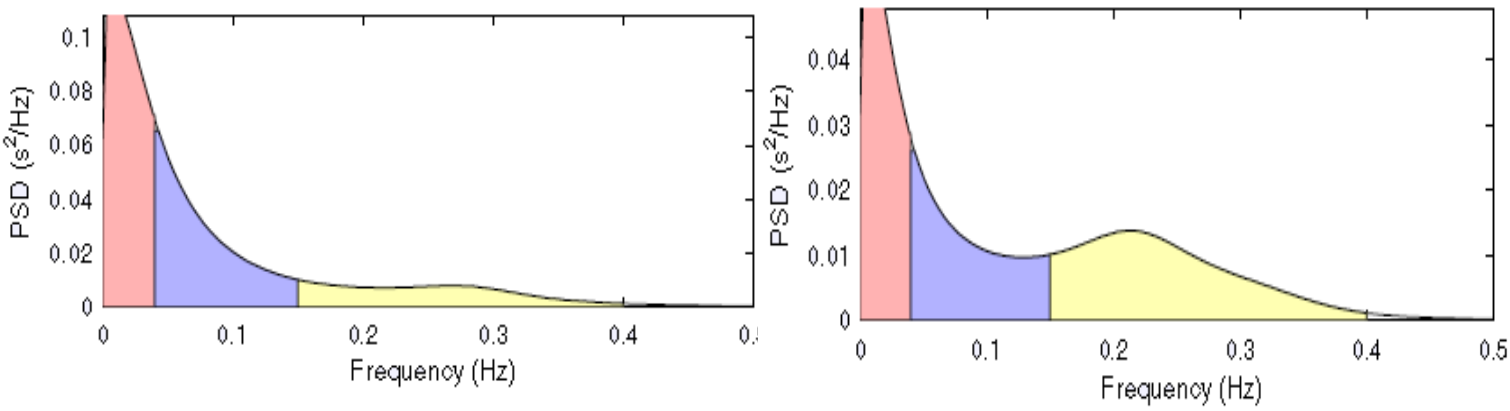

(a) (b)

Figure 2 Typical PSD of heart rate signal : (a) normal subject (b) CAD subject.

The frequency domain plots are divided in to three regions. Each frequency band depicts a physiological processes and pathologies. The initial band is the VLF band followed by LF and then the unshaded portion is the HF range. The VLF variations are associated slow processes like thermal regulation, LF region relates to arterial blood pressure control (both sympathetic and parasympathetic effects) and HF band reflects respiration and parasympathetic activity. From the figures above, it can be observed that the PSD for the CAD subject is approximately half compared to the value of the normal subject for both VLF and LF regions. For the HF region, the PSD is almost the same for normal and CAD. This means that CAD reduces the activity of thermoregulatory and sympathetic systems, but the parasympathetic systems remain unaffected.

The Fourier transform indicates both amplitude and phase of different frequency components which are contained in a time domain signal. A drawback of this method is that

it does not specify the time when these frequencies occur in the signal. So, frequency domain analysis is not preferable to study HR signals. Short Time Fourier Transform , based on a finite length sliding window, solves this issue to a certain degree, but it doesn't work well for rapidly varying signals. HR signals are non-stationary. They are also nonlinear, and hence, conventional time and frequency domain techniques cannot capture all the information contained in the higher harmonics (order greater than 2) of the HR signal. Nonlinear analysis methods and higher order spectrum can capture the higher harmonics information contained in HR signals.

3.3. Nonlinear methods

The theory of nonlinear dynamics is widely to analyze the bio signals, which are nonlinear in nature [Acharya et al., 2004b; 2006; 2007; Faust et al., 2012]. The following are the nonlinear methods that were used in this work: Poincare plots, Recurrence Quantification Analysis (RQA) parameters, Shannon entropy, Approximate Entropy (ApEn), Sample Entropy (SampEn), Higher Order Spectra (HOS) methods, Detrended Fluctuation Analysis (DFA), Empirical Mode Decomposition (EMD), Cumulants, and Correlation Dimension. These methods are briefly explained in the following sub-sections.

3.3.1. Poincare geometry

It is a visual plot, which was adopted from nonlinear methods, to study the behavious of RR interval variability. It depicts the correlation between consecutive intervals in graphical representation. This plot shows the comprehensive every beat to beat variation[Woo et al. 1992 , Kamen et al. 1996]. These plots are studied mathematically by determining the standard deviations of the lengths of RR intervals ($RR(n)$) [Tulppo et al., 1996]. The short term variability (SD1) of the heart signal is measured by the points that are perpendicular to the line-of-identity and long term variability by the points along the line-of-identity. By visually examining the Poincare plot shapes, we can discriminate normal from CAD subjects. In this paper, SD1 parameter was used to detect CAD. Figure 3 shows the Poincare plots of normal (Figure 3(a)) and CAD (Figure 3(b)) subjects. The plots are ellipse shaped and centre-aligned. SD2 describes the long term variability of $RR(n)$ (instantaneous RR), while SD1 indicates the shorter-term variability of $RR(n)$. In the plot for CAD, SD2 and SD1 are very low compared to the normal plot.

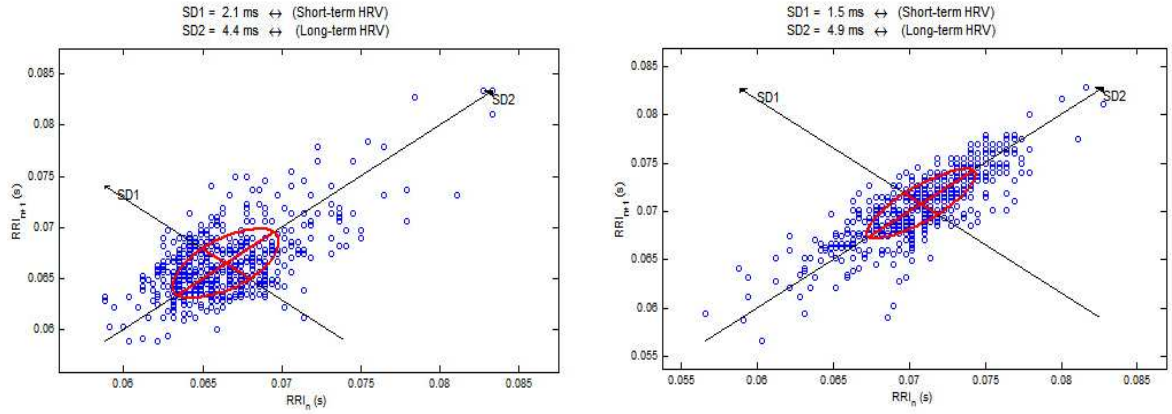

(a) (b)

Figure 3 Typical Poincare plots of HR signals : (a) normal (b) CAD.

3.3.2 Recurrence quantification analysis (RQA)

Recurrence Plot (RP) indicates, for a given instant of time, the times at which path of the phase space meets the same location in the phase space. The duration and counts of recurrences of the dynamical systems are estimated by RQA. It measures the dynamicity and subtle rhythmicity in the HR signal. The RQA parameters evaluate the complexity and non-stationary nature of the time series [Webber et al., (1994), Zbilut et al., (1992) and Marwan et al., (2002)]. Zbilut at al. (2002) showed the usefulness of RQA in detecting randomness and complexity in non-stationary heart beats which cannot be analyzed easily by conventional techniques. In this study, following RQA features were used:

- Mean diagonal line length(<L>or L_{mean}): depicts the average time of forecasting of the system. It can be written as:

$$L_{mean} = \frac{\sum_{l=l_{min}}^{N} lP(l)}{\sum_{i,j}^{N} Pl} \quad (2)$$

- Max line length (L_{max}): It is the largest distance of the diagonal of the RP and is given by:

$$L_{max} = \max(\{l_i ; i = 1,\ldots, N_l\}). \quad (3)$$

Here, N_l indicates the number of diagonal lines in the RP.

- Recurrence Rate (REC): It describes the cloud of recurrence points existing in the plot.

REC is defined as:

$$\mathrm{REC} = \frac{1}{N^2}\sum_{i,j=1}^{N} R_{i,j} \quad (4)$$

- Where $R_{i,j}$ represents the recurrence points, N is the amount of points on phase space path $R_{i,j}$.Determinism (DET): is the portion of $R_{i,j}$ that contribute to the diagonal lines in the plot. It explains the predictability of the dynamical system.

$$\mathrm{DET} = \frac{\sum_{l=l_{min}}^{N} lP(l)}{\sum_{i,j=1}^{N} R(i,j)} \quad (5)$$

Here, $P(l)$ is the distribution in the frequency domain of the diagonal line with lengths l and the minimum diagonal line length is given by l_{min}.

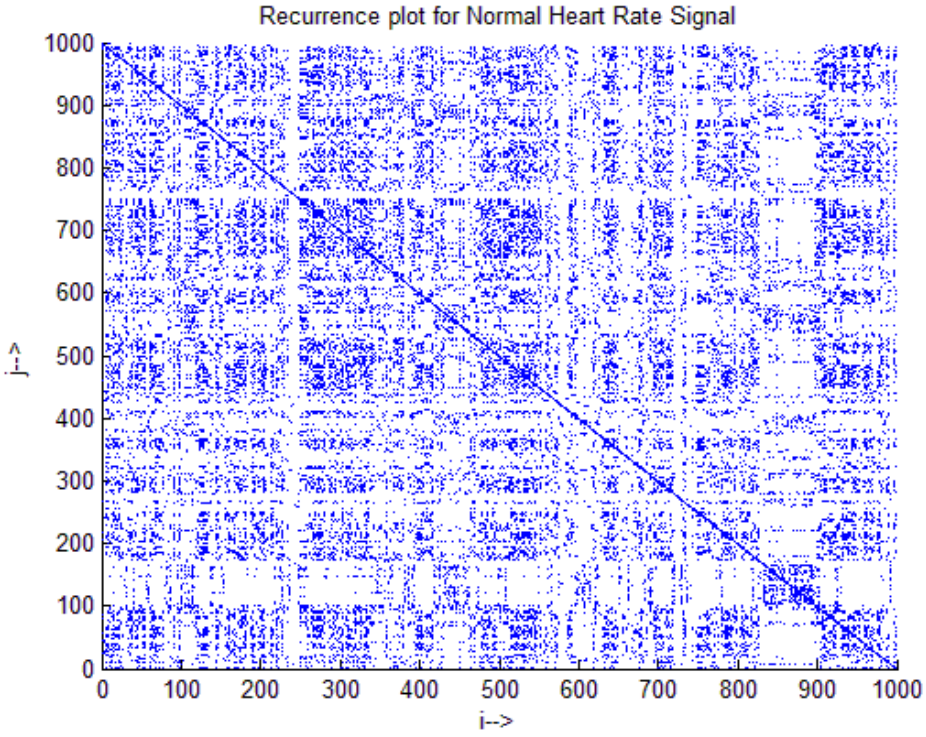

(a)

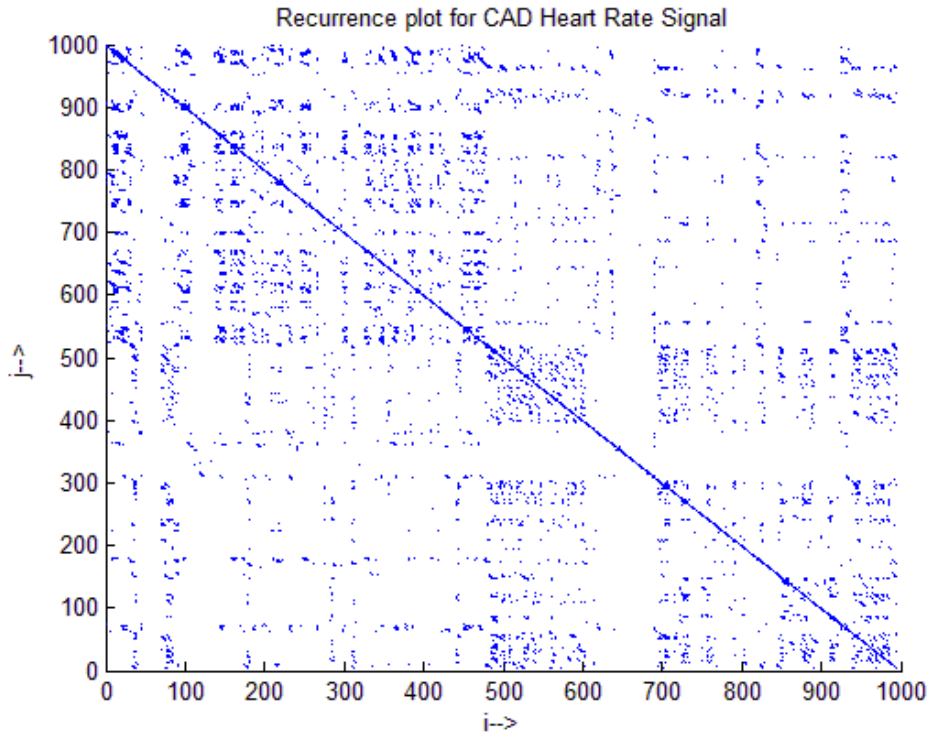

(b)

Figure 4 Typical recurrence plot of HR signal: (a) normal (b) CAD subject.

Figure 4 presents typical RP for normal (Figure 4(a)) and CAD subjects (Figure 4(b)). More variation (dots) is predominant in the normal signal compared to the CAD class. Moreover, there is a more regular pattern in the recurrence plot of CAD. This indicates that there is more rhythmicity with respect to normal subjects.

3.3.3. Approximate entropy (ApEn)

It indicates the fluctuation in the time domain signal [Pincus, 1991]. The value of ApEn is higher for more varying data. Hence, more varying time domain signals will have higher ApEn values, while regular and predictable time series signals will have lower ApEn values. ApEn is given by:

$$ApEn(m,r,N)=\frac{1}{N-m+1}\sum_{i=1}^{N-m+1}\log C_i^m(r)-\frac{1}{N-m}\sum_{i=1}^{N-m}\log C_i^{m+1}(r) \quad (6)$$

where

$$C_i^m(r)=\frac{1}{N-m+1}\sum_{j=1}^{N-m+1}\Theta\left(r-\left\|x_i-x_j\right\|\right) \quad (7)$$

is the correlation integral.

Furthermore, $x_i, x_j x_i, x_j \rightarrow$ Phase space trajectory points,

$N \rightarrow$ Amount of points in the phase space.

$r \rightarrow$ radial length of a circular disc centered at the reference point $x_i x_i$.

$\Theta \rightarrow$ Step function.

In this work, we have used , ' ' is the embedding dimension(m) to 2 and the radial distance r was set to $0.2 \times$ the time series standard deviation [Thakor et al., 2004].

3.3.4. Sample Entropy (SampEn)

It quantifies the complexity in signal [Richman et al., 2000]. Higher values of SampEn describes more irregularities in the time series. It is more refined than ApEn. In order to evaluate sample entropy, continuous matching of points inside the radius '*r*' are done as long as there is match exists. The variables *A(k)* and *B(k)* for all lengths *k* up to '*e*' keep track of all matching templates. It is given by:

$$SampEn(k, r, N) = -\ln \frac{A(k)}{B(k-1)} \tag{8}$$

for $k = 0,1,\ldots, m-1$ with $B(0) = N$, the length of the HR signal, r is taken as 0.2 and m (maximum template length) is set to 2 [Song et al., 2010].

3.3.5. Detrended fluctuation analysis (DFA)

It assess the self-similar properties of short term HR signals [Peng et al., 1996]. The roughness of the signal is indicated by the factor 'α'. This value is close to 1 for normal subjects and may have unique ranges for various cardiac classes.

3.3.6. Correlation Dimension (D2)

D2 is a useful measure of self-similarity of a signal [Grassberger et al., 1983]. According to the algorithm [Grassberger et al., 1983], Correlation integral ($C(r)$) function is constructed first. It was performed by measuring the gap between N pairs of data points and arranging the output dr proportional to r. The gap between a pair of points is estimated by $s(i,j) = |X_i - X_j|$.

C(r) is given by:

$$C(r) = \frac{1}{N^2} \sum_{x=1}^{N} \sum_{y=1, x \neq y}^{N} \Theta(r - |X_x - X_y|) \tag{9}$$

Where, X_x and X_y : indicate phase space trajectory points,

N : total amount of phase space points,

R: radial length of a circular disc centered at X_i-X_j.

Correlation Dimension (D2) can be described by:

$$D2 = \lim_{r \to 0} \frac{\log[C(r)]}{\log(r)} \tag{10}$$

D2 will have higher value, if the RR variations is more and vice versa.

3.3.7. Higher Order Spectrum (HOS)

It is a novel tool for evaluating non-Gaussian and non-stationary bio-signals . It identifies diversions from Gaussianity and phase correlations among frequency components of the signal [Chua et al., 2010]. HOS is more immune to noise and can retain the actual phase information of the signal. The 3rd order statistics is the bispectrum $B(f_1, f_2)$. It is the Fourier transform of the 3rd order correlation of a signal and is given by :

$$B(f_1, f_2) = E[X(f_1)X(f_2)X(f_1 + f_2)] \tag{11}$$

Where, X(f) is the Fourier transform of input X(nT), n is the variable, T is the sampling period, and $E[.]$ is expectation operator. The normalized bispectrum ($B_{norm}(f_1,f_2)$) will have magnitude range 0 to 1 [Nikias et al., 1987; 1993a] and is defined as

$$B_{norm}(f_1, f_2) = \frac{E[X(f_1)X(f_2)X(f_1+f_2)]}{\sqrt{P(f_1)P(f_2)P(f_1+f_2)}} \tag{12}$$

Where $P(f)$ is the power spectrum. In this paper, we have presented discriminating bicoherence and bispectrum plots for normal and CAD HR signals. Both bispectrum and bicoherence plots exhibit symmetry as they are products of three Fourier coefficients.

Various features can be estimated from the bispectrum and few of them are given below:

a) Normalized Bispectral squared entropy1 (P1) is given by

$$P_1 = -\sum_i q_i \log q_i \tag{13}$$

where $q_n = \frac{|B(f_1, f_2)|^2}{\sum_{\Omega} |B(f_1, f_2)|^2}$ and Ω is the region where $f_1 > f_2$ and $f_1 + f_2 < 1$ is as shown in the plot below.

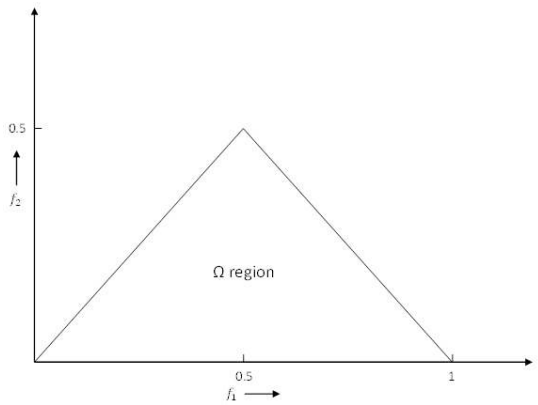

Figure 5: Non-redundant region of bispectrum computation.

The region Ω, is the principal domain used for the evaluation of the bispectrum.

b) Normalised Bispectrum entropy 2 is given by:

$$P_2 = -\sum_i r_i \log r_i \quad (14)$$

where $r_n = \frac{|B(f_1,f_2)|^3}{\sum_\Omega |B(f_1,f_2)|^3}$

Ω = is the principal domain shown in Figure 5.

c) The mean bispectrum magnitude is:

$$M_{ave} = \frac{1}{L}\sum_\Omega \left|B(f_1, f_2)\right| \quad (15)$$

M_{ave} can be used to distinguish between two classes.

d) The bispectrum phase entropy is:

$$P_e = \sum_n p(\Psi_n) \log p(\Psi_n) \quad (16)$$

Where:

$$p(\Psi_n) \text{ is } p(\Psi_n) = \frac{1}{L}\sum_\Omega 1\left(\Phi\left(b(f_1, f_2)\right) \in \Psi_n\right) \quad (17)$$

And:

$$\Psi_n = \{\Phi / -\pi + 2\pi n / N \le \Phi < -\pi + 2\pi(n+1)/N, n = 0,1,.....N-1. \quad (16)$$

Here, L indicates the amount of points in the principal region and Φ is the bispectrum phase angle. The function 1(.) yields 1 if ϕ (phase angle) falls inside bin Ψ_n .

e) The weighted center of bispectrum (WCOB) is defined as:

$$wcobx = \frac{\sum_{\Omega} iB(i,j)}{\sum_{\Omega} B(i,j)} \qquad wcoby = \frac{\sum_{\Omega} jB(i,j)}{\sum_{\Omega} B(i,j)} \tag{17}$$

where, i and j are frequency bin index in the non-redundant region.

Figure 6(a) presents the contour plots of bispectrum for normal and CAD heart rate signal (Figure 6(b)) respectively. By visually examining these plots, we can distinguish between normal and CAD subjects clearly. In the bispectrum plot of the normal subject (Figure 6(a)), there are peaks concentrated in the centre, while for CAD subject (Figure 6(b)), the peaks are present throughout the plot and spread throughout the frequency spectrum.

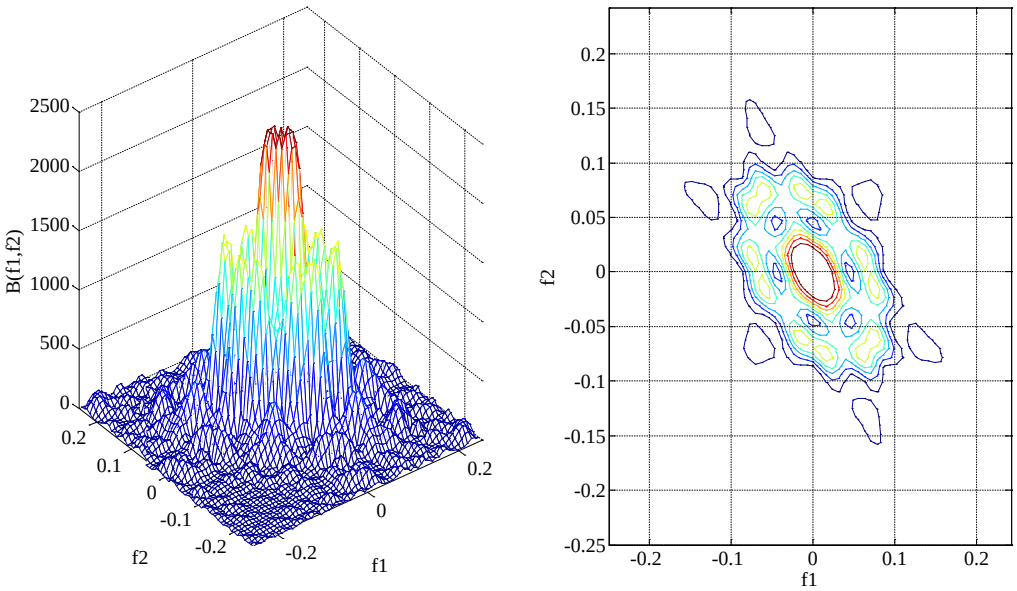

(a)

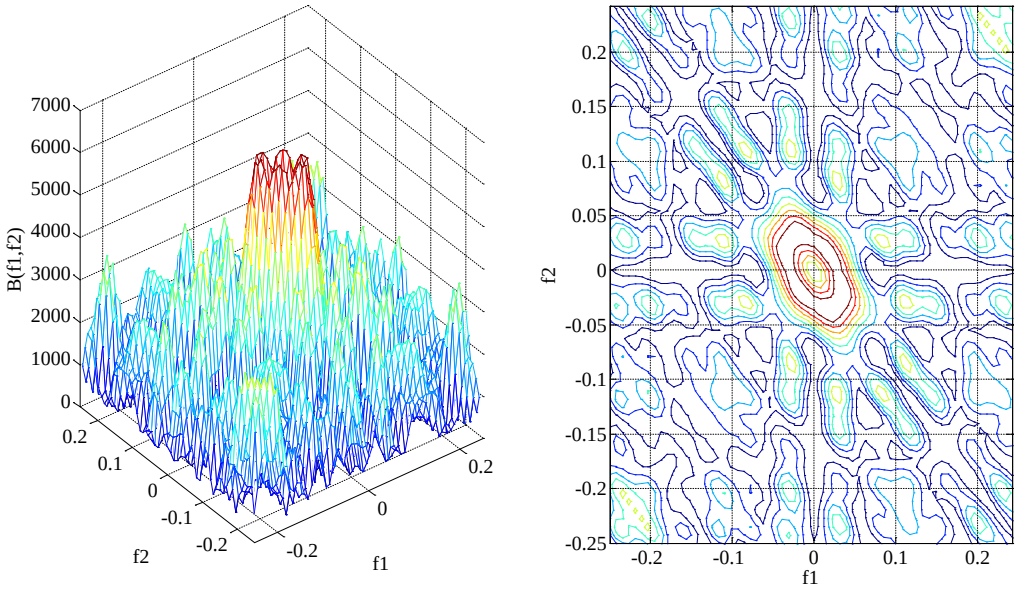

(b)

Figure 6 Typical Bispectrum and its contour plots for (a) Normal and (b) CAD subjects.

3.3.8. Cumulant Computation

It is not easy to analyze the nonlinear and non-stationary behavior time series using 1st and 2nd order statistics [Nikias, 1993b]. So, third order cumulant which is a third order correlation derived from HOS can be used for HR signals. It has been successfully implemented to differentiate automatically control, ictal and interictal EEG signals [Acharya et al., 2011].

Let $\{x_1, x_2, x_3, ...x_k\}$ indicate a k dimensional random process of zero mean value . Its moments are given by [Nikias, 1993]:

$$m_1^x = E\left[x(n)\right] \tag{18}$$

$$m_2^x(i) = E\left[x(n)x(n+i)\right] \tag{19}$$

$$m_3^x(i,j) = E\left[x(n)x(n+i)x(n+j)\right] \tag{20}$$

$$m_4^x(i,j,k) = E\left[x(n)x(n+i)x(n+j)x(n+k)\right] \tag{21}$$

where m_1^x, m_2^x, m_3^x and m_4^x are 1st , 2nd , 3rd and 4th order moments, $E[.]$ indicates the expectation operator, and time lag parameters are I, j. Using moments, cumulants are evaluated as [Nikias, 1993]:

$$C_1^x = m_1^x \tag{22}$$

$$C_2^x = m_2^x(i) \tag{23}$$

$$C_3^x = m_3^x(i, j) \tag{24}$$

$$C_4^x = m_4^x(i, j, k) - m_2^x(i)m_2^x(j-k) - m_2^x(k-i) - m_2^x(k)m_2^x(i-j) \tag{25}$$

where C_1^x, C_2^x, C_3^x and C_4^x are the 1st, 2nd , 3rd and 4th order cumulants respectively. In the current study the third order cumulant is used for the analysis of HR signals. Figure 7(a) shows the 3rd order cumulant plot and its contour plot for normal HR signal and Figure 7(b) for CAD HR signal.

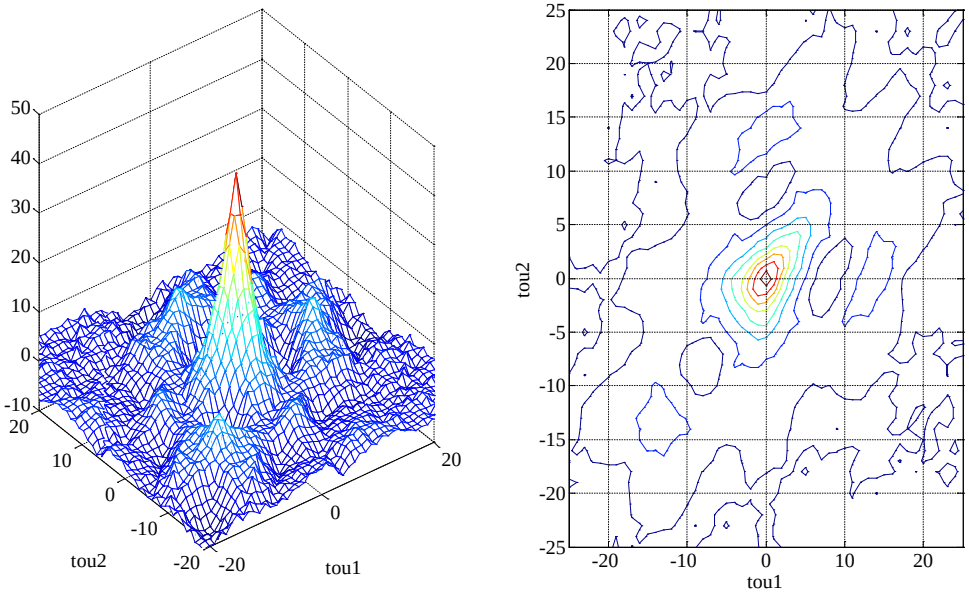

(a)

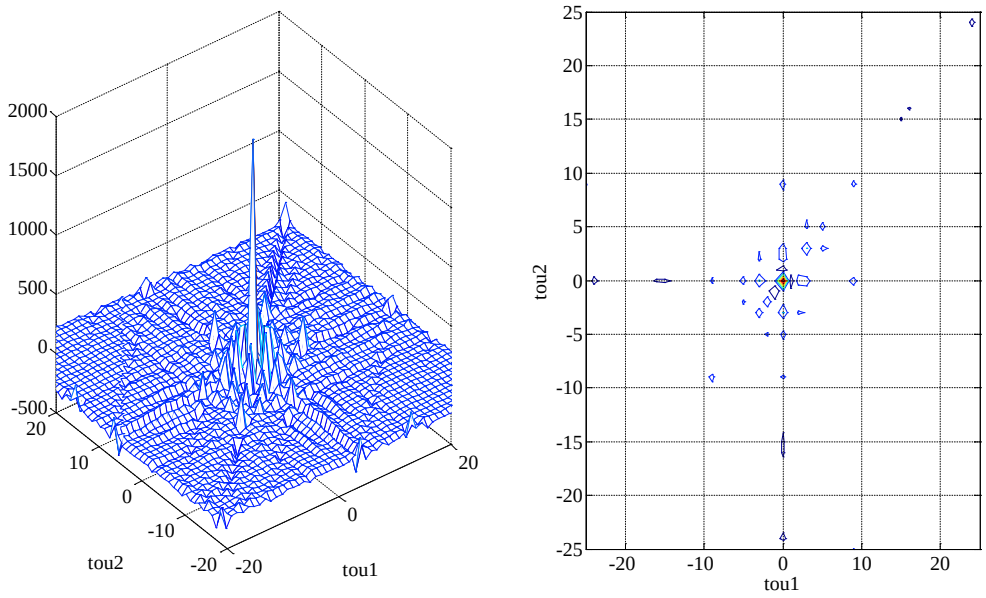

(b)

Figure 7 Typical third cumulant and its contour plots: (a) normal and (b) CAD subject.

3.3.8 Empirical Mode Decomposition (EMD)

It is a direct, adaptive and data dependent model for nonlinear signal analysis. It does not assume linearity and stationarity conditions [Huang et al., 1998]. Any complicated signal can be decomposed into a group of Intrinsic Mode Functions (IMFs) which are AM and FM modulated waveforms. The decomposition is based on local time and scale of the signal. Martis et al. (2012) applied EMD for the analysis for EEG signals of control, preictal and ictal classes. Figure 8 presents eight IMFs of typical normal (Figure 8(a)) and CAD (Figure 8(b)) HR signal. Various important features can extracted from these IMFs to classify the normal and CAD HR signals.

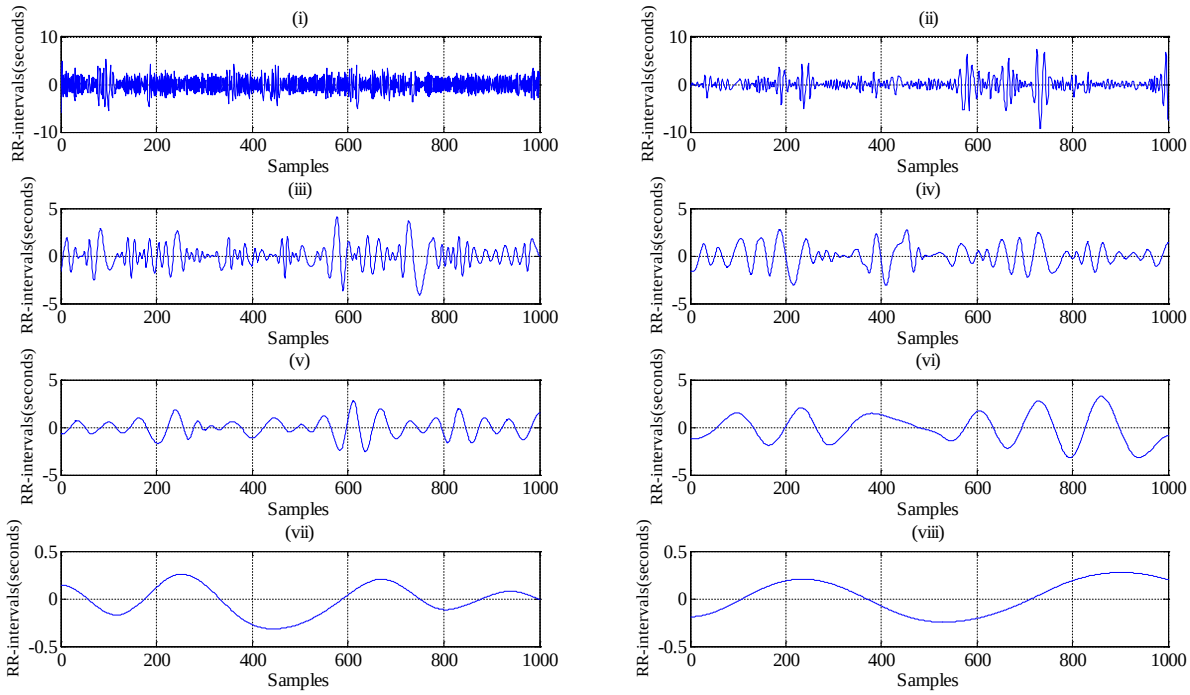

(a)

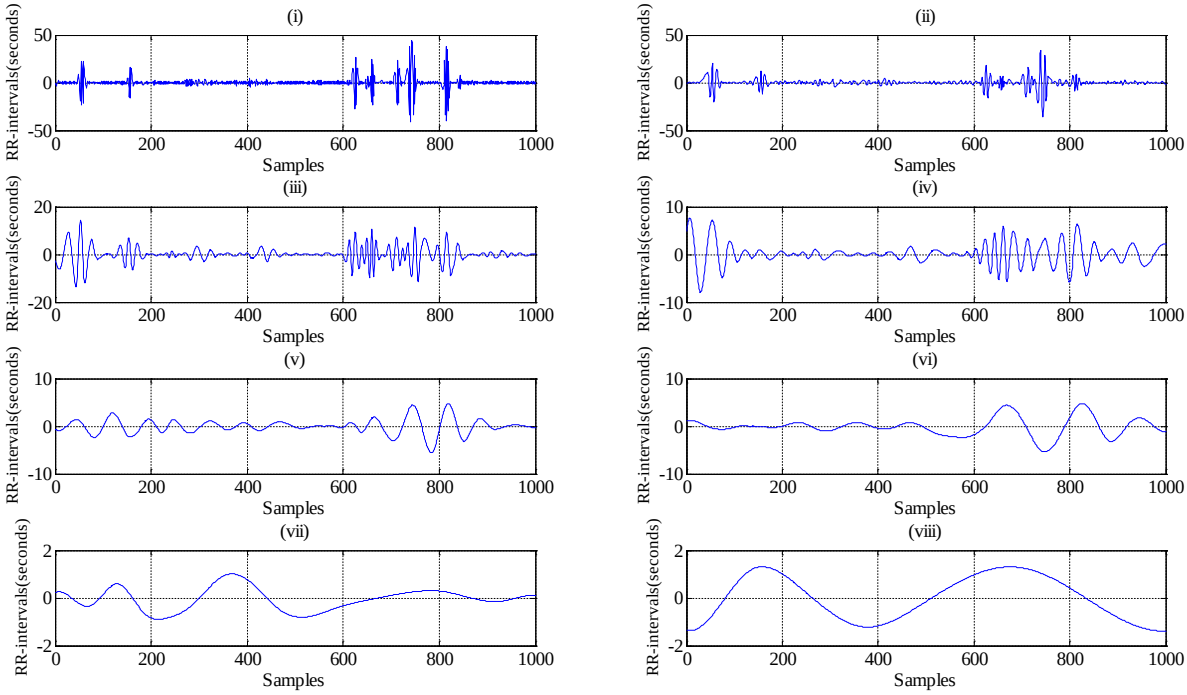

(b)

Figure 8 Typical IMFs extracted from EMD decomposition for HR signal: (a) normal and (b) CAD.

4. Results

Results of time domain, frequency domain and nonlinear techniques are presented in this section. Table1 shows the feature values (Mean ± Standard Deviation(SD)) of the time domain parameters of normal and CAD HR signals. In this work, four time domain features were found to be clinically significant ($p<0.05$). They are mean HR, RMSSD, NN50 and pNN50 (listed in Table 1).

Table 1 Results of time domain analysis.

Features	Normal (Mean±SD)	CAD (Mean±SD)	p-value
Mean HR	52.9±6.62	45.6±16.1	0.0008
RMSSD	44.5 ±16.0	72.7 ± 99.0	0.021
NN50	187±145	68.3 ± 103	< 0.0001
pNN50	21.5 ± 15.7	7.31 ± 11.5	< 0.0001

The clinically significant features like NN50 and pNN50, have lower values for the CAD subjects with respect to the normal. The difference is more than order 2. The next significant parameter, mean HR, is lower for CAD signals than for normal subjects. RMSSD is higher for CAD than for normal subjects.

In the frequency domain analysis, we have also obtained four clinically significant features for LF to HF. The ratio LF to HF indicates sympathetic parasympathetic balance of heart. Table 2 shows frequency domain analysis results for CAD and normal heart rate signals.

Table 2 Results of frequency-domain analysis.

Features	Normal (Mean ± SD)	CAD (Mean ± SD)	p-value
LF/HF	2.93±2.46	943±3.109E+03	0.013

In our work, all the four frequency domain features have higher values for the CAD than for normal subjects. We have used a variety of nonlinear parameters for analysis. Table 3 gives the summary of these nonlinear features.

Table 3 Results of nonlinear analysis.

Features	Normal (Mean±SD)	CAD (Mean±SD)	p-value
SD1	31.5 ± 11.3	52.5 ±69.4	0.014
L_{mean}	14.3±5.57	39.1± 45.5	< 0.0001
Max line length (L_{max})	378± 229	513±290	0.0044
Recurrence rate (REC)	38.5 ±10.5	55.7±18.4	< 0.0001
Determinism (DET)	98.4 ± 1.10	99.4 ± 0.772	< 0.0001
ApEn	1.33 ± 0.121	1.05 ±0.288	< 0.0001
SampEn	1.47 ±0.225	1.04 ±0.390	< 0.0001
DFA (α1)	1.15 ± 0.209	0.933±0.407	0.0002
Correlation dimension (D2)	3.41 ± 1.27	1.07 ± 1.16	< 0.0001

SD1 measures the short term variability of the heart signal. This value (SD1) for CAD signals is higher than for normal signals. Thus, SD1 reflects the fast variations brought by CAD on heartbeat. The next four parameters, L_{mean}, L_{max}, REC and DET, belong to the RQA analysis. The values of these four parameters are high for the CAD group. For the first three values, the increase was significant while for the last parameter, CAD group showed only a slight increase compared to the normal group. The higher RQA parameters indicate more order or less variation in the signal. Hence, higher values of RQA parameters correctly indicate that the variation in CAD is less compared to normal subjects.

Entropy parameters (ApEn and SampEn) showed higher values for normal HR signal compared to CAD . ApEn value will be small for cardiac impairment cases. It is evident from Table 3 that for the CAD signal, ApEn takes a value much less than normal subjects. SampEn parameter also showed low value for CAD. In general, the results showed a reduction in entropy-based parameters for CAD. That means the entropy is reduced due to the reduction in HRV for CAD.

The DFA parameter takes a large value as the input time series signal is more rhythmic. Accordingly, for normal subjects, we obtained larger values for DFA compared to CAD subjects.

D2 is a quantitative measurement which indicates the nature of the path in a phase space. D2 decreases as the beat-to-beat variation decreases [Acharya et al., 2004a; 2004b]. The D2 value obtained for the CAD class is about one-third of that for the normal class.

Table 4 gives details of HOS parameters which were extracted, and the corresponding p-value. Except phase entropy (P_e), all HOS parameters showed higher values for the CAD class. CAD, with its high beat-to-beat variability, results in higher values for HOS parameters. The disorder in the HR signals of a CAD subject shows itself as an increase in the information content in the higher harmonics of the HR signal. CAD brings short term fast beat-to-beat variability, thus causing the signal to contain extra information in higher harmonics compared to normal HR signals.

Table 4 Results of HOS analysis.

Features	Normal (Mean ± SD)	CAD (Mean ± SD)	p-value
P_1	0.427 ±0.151	0.541 ±0.310	0.0074
P_2	0.246±0.126	0.405 ± 0.300	< 0.0001
M_{avg}	0.392 ±0.481	134± 393	0.0052
P_e	3.55 ± 5.488E-02	3.12 ± 0.867	< 0.0001
Wcob1	26.3 ± 18.0	39.5± 29.3	0.0023
Wcob3	34.7 ± 10.6	43.2 ±21.4	0.0038
Wcob4	10.3 ±2.87	12.8 ± 7.31	0.0086

5. Discussion

Goldberger et al. (1987) showed that under normal conditions our heart is not a periodic oscillator. Since then, several nonlinear methods were proposed to quantitatively measure the heart rate variations [Goldberger et al., 1987; Pincus 1991]. Nonlinear parameters like recurrence percentage, fractal dimension, etc. were significantly different for normal and CAD subjects of the ECG signals [Antanavicius et al., (2008)]. Manis et al. (2007), Laitio et al. (2004) and Qtsuka et al. (2009) used correlation dimension and entropy features on heart rate signals to diagnose CAD. Karamanos et al. (2006) analyzed HR signals using DFA and showed that the self similarity nature of heart rate signals decreased in CAD subjects.

Table 5 Summary of studies conducted in automated detection of CAD and normal classes.

Authors	Base signal/Techniques Used	Classifiers	Accuracy
Karimi et al. (2005)	Heart sound, Wavelet analysis	Neural network	85%
Arafat et al. (2005)	ECG Stress Signals with Probabilistic Neural Networks	Fuzzy Inference Systems	80%
Lee et al. (2007)	HRV, Linear and Nonlinear Parameters	SVM Classifier	90%
Kim et al. (2007)	HRV, Multiple Discriminant Analysis with linear and nonlinear feature	Multiple Discriminant Analysis	75%
Zhao et al. (2008)	Diastolic murmurs, EMD-Teager Energy Operator	Back Propagation Neural Network	85%
Lee et al. (2008)	HRV, carotid arterial wall thickness	CPAR and SVM	85 - 90%
Babaoglu et al. (2010a)	EST-ECG, PSO+GA	SVM	81.46%
Babaoglu et al. (2010b)	EST-ECG, PCA	SVM	79.71%
Dua et al. (2012)	Nonlinear features +PCA	MLP	89.5%
Giri et al. (2012)	HR signals , ICA	GMM	96.8%
This work	HRV	No classification done	We have proposed unique linear and nonlinear feature

							ranges for CAD and normal and also proposed unique plots; No accuracy reported

Table 5 shows the summary of the studies conducted for the automated diagnosis of CAD and normal HR signals. Karimi et al. (2005) presented classification result of 85% for CAD identification using the combination of artificial neural networks and wavelet features extracted from the heart sounds. ECG stress signals combined with fuzzy and probabilistic methods were effectively used to detect CAD with an accuracy of 80% [Arafat et al., 2005]. Various linear and non-linear features were derived from heart rate signals in the left lateral, supine, and right lateral position [Lee et al., 2007]. In their work SVM yielded the highest accuracy of 90% compared to Bayesian classifiers, *CMAR*, and *C4.5.* The same group used the HRV features of different postures and carotid arterial wall thickness as features and classified the normal and CAD subjects with an accuracy of 85% to 90% using CAPAR and SVM classifier [Lee et al., 2008]. Classification was performed into control, angina pectoris and acute coronary syndrome using linear and nonlinear features of HR signals [Kim et al., 2007]. They reported an accuracy of 75%, and classified angina pectoris group with a sensitivity of 72.5% and specificity of 81.8%. Their system was able to classify people suffering from acute coronary syndrome with a sensitivity of 84.6% and specificity of 91.5%. Features extracted from heart murmurs using EMD – Teager energy operator automaticaly diagnosed normal and CAD subjects with an accuracy of 85% [Zhao et al., (2008)].

Binary Particle Swarm Optimization coupled with genetic algorithm applied on exercise data to detect the CAD yielded an accuracy of 81.4% using SVM classifier using twenty three features [Babaoglu et al., 2010a]. Same group reduced the twenty three features of the exercise stress test data to eighteen features and obtained an accuracy of 79.71% using SVM classifier (Babaoglu et al. (2010b)). Recently, Giri et al. (2012) classified normal and CAD classes using HR as base signal. Discrete wavelet transform (DWT) coefficients were subjected to data reduction using Independent Component Analysis (ICA). These ICA coefficients were classified using Gaussian Mixture Model (GMM) with an accuracy of 96.8%. The nonlinear features extracted from the HR signals were fed to

principal component analysis (PCA) for data reduction[Dua et al., 2012]. These PCA coefficients coupled with multilayer perceptron (MLP) method resulted in the highest classification accuracy (89.5%) to classify normal and CAD heart rate signals.

Unique ranges have been proposed for time, frequency and nonlinear features for normal and CAD HR signals. These extracted parameters can be used for automated detection of CAD using HR signals. The practical relevance of this study can be improved by using more diverse data form a wider range of subjects. It is risky to obtain the ECG signals during exercise from CAD affected subjects. Hence, signals like heart murmur, ECG stress signals, and HRV signals are more preferred to detect the normal and CAD classes.

The time domain analysis is not robust, due to the influence of artifacts and noise. The temporal information of the frequency content cannot be provided by the Fourier transform. The HR signal is a nonlinear signal and the information content in the higher harmonics of the signal can only be completely captured by nonlinear analysis methods. Hence, in this work, we evaluated the ranges of several nonlinear features extracted from normal and CAD affected subjects. We found that the RQA parameters, such as L_{mean}, L_{max}, REC and DET, were higher for CAD subjects indicating more rhythm. Since the activity of CAD subjects is less, similar signal patterns repeat or recur more frequently compared to the normal subjects. Hence, the parameter REC has higher value for CAD subjects. Similarly, the value of the determinism parameter or DET is higher for CAD subjects. This is again is due to the fact that CAD subjects are less active than normal subjects. The same processes occur very frequently and thus it is easier to determine the HR signal. The entropy based parameters, ApEn and SampEn, are lower for CAD subjects indicating lower entropy (less activity due to impairment) for CAD. Almost all HOS parameters showed higher values for the CAD group, indicating the presence of higher frequency content in the CAD signals.

6. Conclusion

CAD is one of the prime reasons for the majority of cardiac deaths worldwide. In this work, we analyzed HR signals which were obtained from ECG data recorded from normal and CAD subjects. In our work, we have made an attempt to analyze both normal and CAD heart rate signals in time, frequency and non-linear domain. Our results show that HR signals are less variable in CAD subjects, compared to the normal subjects. We have

proposed unique ranges for features in in various domains. Highly discriminative recurrence, Poincare, HOS plots have been presented to differentiate normal and CAD heart rate signals. These ranges of features and unique plots can be used in future to identify these two classes.

Acknowledgements: Authors thank Ms Ratna Yanti for running the codes and compiling the results and Thanjuddin Ahmad for providing the data. HRV analysis Software, Biomedical Signal Analysis Group, University of Kuopio, Finland for providing the software.

References

1. U.R. Acharya, P.S. Bhat, S.S.Iyengar, A. Rao, S. Dua, Classification of heart rate using artificial neural network and fuzzy equivalence relation, Pattern Recognition 36 (2003)61–68
2. U. R. Acharya, J.Suri, A. E. Jos. Spaan, S. M. Krishnan, Advances in cardiac signal processing, Springer VerlagGmBh Berlin Heidelberg (2007).
3. U. R. Acharya, K. P.Joseph, N. Kannathal, C. Lim, J. Suri, Heart rate variability: a review, Medical and Biological Engineering and Computing 44 (2006) 1031-1051.
4. U.R. Acharya, N. Kannathal, S.M. Krishnan, Comprehensive analysis of cardiac health using heart rate signals, Physiological Measurement 25 (2004a) 1139-1151.
5. U. R. Acharya, N. Kannathal, O. Sing, L. Ping, T. Chua, Heart rate analysis in normal subjects of various age groups, Biomedical Engineering Online 3 (1) (2004b) 24.
6. U. R. Acharya, S. V. Sree, J. S. Suri, Automatic detection of epileptic EEG signals using higher order cumulants, International Journal of Neural Systems, 21(5) (2011) 403-414.
7. H. Akaike, Fitting autoregressive models for prediction, Annals of the Institute of Statistical Mathematics 21(1969) 243-7
8. H. Akike, A new look at statistical model identification IEEE transaction on Automatics Control 19 (1974) 716-23.

9. S. Akselrod, D. Gordon, F. A. Ubel, D.C. Shannon, A. C. Berger, R.J. Cohen, Power Spectrum analysis of heart rate fluctuation: A quantitative probe of beat-to-beat cardiovascular control, Science (1981) 213:220-2.
10. B. Anita, F. S. Schlindwein, A. P. Rocha , A. Leite, A study on the optimum order of autoregressive models for heart rate variability, Physiological Measurements23 (2002) 324-336.
11. K. Antanavicius , A. Bastys, J. Bluzas, L. Gargasas, S. Kaminskiene, G. Urbonaviciene, A. Vainoras , Nonlinear dynamics analysis of electrocardiograms for detection of coronary artery disease, Comput Methods Programs Biomed. 92(2) (2008) 198-204.
12. S. Arafat, M. Dohrmann and M. Skubic, Classification of coronary artery disease stress ECGs using uncertainty modeling, Congress on Computational Intelligence Methods and Applications (2005).
13. S. Arica, N. F. Ince, A. Bozkurt, A. Birand, A. H. Tewfik, Predictability of baroreflex sensitivity by phenyl ephrine injection via frequency domain indices computed from heart rate and systolic pressure signals during deep breathing, Biomedical Signal Processing and Control 5 (4) (2010) 292-298
14. I. Babaoglu, O. Findik, E. Ülker, A comparison of feature selection models utilizing binary particle swarm optimization and genetic algorithm in determining coronary artery disease using support vector machine. Expert Syst. Appl. 37,(2010a) 3177-3183.
15. I. Babaoglu, O. Findik, M. Bayrak, Effects of principle component analysis on assessment of coronary artery diseases using support vector machine, Expert Syst. Appl. 37, (2010b) 2182-2185.
16. J.T. Bigger Jr, J.L. Fleiss, R.C. Steinman, L.M. Rolnitzky, W.J. Schneider, P.K. Stein, RR variability in healthy, middle-aged persons compared with patients with chronic coronary heart disease or recent acute myocardial infarction, Circulation 91 (1995) 1936 -1943.
17. R.D. Brook, B.Franklin, W.Cascio, Y. Hong, G. Howard, M.Lipsett, R. Luepker, M. Mittleton, J. Samet, S.C. Smith, I. Tager, Air Pollution and Cardiovascular Disease, Circulation, 109 (2004) 2655-2671.

18. R.M. Carney, K.E. Freedland, P.K. Stein, J.A. Skala, P. Hoffman and A.S. Jaffe, Change in heart rate and heart rate variability during treatment of depression in patients with coronary artery disease, Psychosomatic Medicine 62 (2000) 639-647.
19. K. C. Chua, V. Chandran, U. R. Acharya, C. M. Lim, Cardiac state diagnosis using higher order spectra of heart rate variability, Journal of Medical Engineering and Technology 32(2) (2006) 145-155.
20. K. C. Chua, V. Chandran, U. R. Acharya, C. M. Lim, Computer- based analysis of cardiac state using entropies, recurrence plots and Poincare geometry, Journal of Medical & Engineering Technology 2 (4)(2008) 263-272.
21. K. C. Chua, V. Chandran, U. R. Acharya, C. M. Lim, Application of higher order statistics/spectra in biomedical signals - A Review, Medical Engineering and Physics 32(7) (2010) 679-689.
22. M. Cohen, D. L. Hudson, P. C. Deedwania, Heart rate variability and cardiovascular mortality, Engineering in Medicine and Biology Magazine, IEEE 15 (1996) 97-102.
23. D. G. Giri, U. R. Acharya, R. J. Martis, V. S. Sree, T. C. Lim, T. V. I. Ahamed, J. S. Suri, Automated Diagnosis of Coronary Artery Disease Affected Patients Using LDA, PCA, ICA and Discrete Wavelet Transform, Knowledge Based Systems, (2012).
24. S. Dua, X. Du, V. S. Sree, Ahmed, T. V. I., "Novel classification of coronary artery disease using heart rate variability analysis", Journal of Mechanics in Medicine and Biology, 12(4), (2012) 1240017-1 -19.
25. O. Faust, U. R. Acharya, S. M. Krishnan, L. C. Min. Analysis of cardiac signals using spatial filling index and time-frequency domain. BioMedical Engineering Online, pages –, September 2004.
26. O. Faust, M. G. Bairy. Nonlinear analysis of physiological signals: A review. Journal of Mechanics in Medicine and Biology, –:In press, 2012
27. J. Fell, K. Mann, J. Roschke, M. S. Gopinathan, Nonlinear analysis of analysis of continuous ECG during sleep I, Reconstruction BiolCybernat 82 (2000) 477-483
28. A.L. Goldberger, B.J. West, Application of non-linear dynamics to clinical cardiology, Annals of the New York Academy of Sciences, 504 (1987) 195–213
29. P. Grassberger, I. Procassia, Measuring the strangeness of strange attractors, Physica D 9 (1983) 189-208.

30. A.R. Gujjar, T.N. Sathyaprabha, D. Nagaraja, K. Thennarasu and N. Pradhan, Heart rate variability and outcome in acute severe stroke: Role of power spectral analysis, Neurocritical Care 1(3) (2004) 347-354.
31. J. Hayano, Y. Sakakibara, A.Yamada, N.Ohte, T. Fujinami, K. Yokoyama, Y. Watanabe and K. Takata, Decreased magnitude of heart rate spectral components in coronary artery disease. Its relation to angiographic severity, Circulation 81 (1990) 1217-1224.
32. http://www.biopac.com/ (Last accessed in July 2011).
33. N. E. Huang, Z. Shen, S. R. Long, M. C. Wu, H. H. Shih, Q. Zheng, N-C. Yen, C. Tung, H. H. Liu, The empirical mode decomposition and the Hilbert spectrum for nonlinear and nonstationary time series analysis, *Proc. R. Soc. Lond. A* 454 (1998) 903–995.
34. H.V. Huikuri, T.H. Makikallio, C.K. Peng, A.L. Goldberger, U. Hintze and M. Moller, Fractal correlation properties of R-R interval dynamics and mortality in patients with depressed left ventricular function after an acute myocardial infarction, Circulation 101 (2000) 47–53.
35. Y. Isler. M. Kuntalp, Combining classical HRV indices with wavelet entropy measures improves to performance in diagnosing congestive heart failure, Computers in Biology and Medicine 37 (2007) 1502-1510.
36. P.W. Kamen, H. Krum, A.M.Tonkin, Poincare plot of heart rate variability allows quantitative display of parasympathetic nervous activity, Clinical science 91 (1996) 201-208.
37. K. Karamanos, S. Nikolopoulos, G. Manis, A. Alexandridi, K. Hizanidis and S. Nikolakeas, Block entropy analysis of heart rate variability signals, International Journal of Bifurcation and Chaos 16(7) (2006) 2093-2101.
38. M. Karimi, R. Amirfattahi, S. Sadri and S.A. Marvasti, Non-invasive detection and classification of coronary artery occlusions using wavelet analysis of heart sounds with neural networks, 3rd IEE International Seminar on Medical Applications of Signal Processing (2005) 117-120.

39. W., Kim, S., Jin, Y., Park, H., Choi, A study on development of multi-parametric measure of heart rate variability diagnosing cardiovascular disease, IFMBE Proceedings. 14, (2007) 3480-3483.
40. T.T. Laitio, H.V. Huikuri, T.H. Makikallio, J. Jalonen, E.S.H. Kentala, H. Helenius, O. Pullisaar, J. Hartiala and H. Seheinin, The breakdown of fractal heart rate dynamics predicts prolonged postoperative myocardial ischemia, Anesthesia& Analgesia 98 (2004) 1239-1244.
41. K.M. Lavoie, R.P. Fleet, C. Laurin, A. Arsenault, S.B. Miller and S.L. Bacon, Heart rate variability in coronary artery disease patients with and without panic disorder, Psychiatry Research 128(3) (2004) 289-299.
42. H. G. Lee, K. Y. Noh, K. H. Ryu, A data mining approach for coronary heart disease prediction using HRV features and carotid arterial wall thickness. International Conference on Biomedical Engineering and Informatics. 1, (2008) 200-206.
43. H. G. Lee, K. Y., Noh, K. H., Ryu, Mining Biosignal Data: Coronary Artery Disease Diagnosis Using Linear and Nonlinear Features of HRV. PAKDD Workshops (2007) 218-228.
44. F. Lombardi, Chaos Theory, Heart Rate Variability, and Arrhythmic Mortality, Circulation 101 (1) (2000) 8-10.
45. G. Manis, S. Nikolopoulos, A. Alexandridi and C. Davos, Assessment of the classification capability of prediction and approximation methods for HRV analysis, Computers in Biology and Medicine 37 (2007) 642-654.
46. R.J. Martis, U. R. Acharya, J. H. Tan, A. Petznick, R. Yanti, C. K. Chua, E. Y. K. Ng, L. Tong, Application of empirical mode decomposition (EMD) for automated detection of epilepsy using EEG signals, International Journal of Neural Systems (2012) (In Press).
47. N. Marwan, N. Wessel, U. Meyerfeldt, A. Schirdewan and J. Kurths, Recurrence plot based measures of complexity and its application to heart rate variability data, Physics Review E 66(2) (2002) 026702.
48. C. L. Nikias, A. P. Petropulu, Higher-order spectra analysis: A nonlinear signal processing framework (Englewood Cliffs, HJ: PTR Prentice Hall) (1993a)

49. C. L. Nikias, M. R. Raghuveer, Bispectrum Estimation: A digital signal processing frame work, Proceedings of IEEE , 75(1987) 869-890
50. Nikias, C.L., Higher-order spectral analysis, Engineering in Medicine and Biology Society, 1993. Proceedings of the 15th Annual International Conference of the IEEE , (1993b), 319.
51. S. Nikolopoulos, A. Alexandridi, S. Nikolakeas and G. Manis, Experimental analysis of heart rate variability of long-recording electrocardiograms in normal subjects and patients with coronary artery disease and normal left ventricular function, Journal of Biomedical Informatics 36 (2003) 202–217.
52. M. I. Owis, A. H. Abou-Zied, A. B. M. Youssef, Y. M. Kadah, Study of features on nonlinear dynamical modeling in ECG arrhythmia detection and classification, IEEE Trans Biomed Eng 49(7)(2002) 733-6
53. J. Pan and W.J. Tompkins, A real-time QRS detection algorithm, IEEE Transactions on Biomedical Engineering 32 (3) (1985) 230-236.
54. C.K. Peng, S. Havlin, J.M. Hausdorf, J.E. Mietus, H.E. Stanley, A.L. Goldberger , Fractal mechanisms and heart rate dynamics, J Electrocardiol 28 (Suppl) (1996) 59-64
55. S. M.Pincus, Approximate entropy as a measure of system complexity, Proceedings of National Academic Science, USA, 88 (1991) 2297-2301.
56. K. Qtsuka, G. Cornélissen and F. Halberg, Circadian rhythmic fractal scaling of heart rate variability in health and coronary artery disease, Clinical Cardiology 20(7) (2009) 631-638.
57. J. S. Richman, M. J.Randall, Physiological time-series analysis using approximate entropy and sample entropy, Am J Physiol Heart Circ Physiol 278(2000)H2039-H2049
58. J.A. San Roman, I. Vilacosta, J.A. Castillo, M.J. Rollan, M. Hernandez, V. Peral V, I. Garcimartín, M.M. de la Torre and F. Fernández-Avilés, Selection of the optimal stress test for the diagnosis of coronary artery disease, Heart 80(4) (1998) 370–376.
59. A. Schumacher, Linear and Nonlinear Approaches to the Analysis of R-R Interval Variability, Biological Research For Nursing 5 (3) (2004) 211-221.
60. A. Schumann, N. Wessel, A. Schirdewan, K.J. Osterziel and A. Voss, Potential of feature selection methods in heart rate variability analysis for the classification of different cardiovascular diseases, Statistics in Medicine 21(15) (2002) 2225-2242.

61. E.N. Silber and L.N. Katz, Heart Disease, p. 498 (Macmillan Publishing Co, New York)(1975).
62. Y. Song, P. Liò, A new approach for epileptic seizure detection: sample entropy based feature extraction and extreme learning machine, Journal of Biomedical Science and Engineering 3 (6) (2010) 556-567.
63. D. Steinberg, A. M. Gotto, Preventing Coronary Artery Disease by Lowering Cholesterol Levels, JAMA, 282(21) (1999) 2087-2088.
64. Y. Sun, K. L. Chan, S. M. Krishnan, Arrhythmia detection and recognition in ECG signals using nonlinear techniques, Ann Biomed Eng (2000) 28(1) S-37.
65. Task Force of the European Society of Cardiology and North American Society of Pacing and electrophysiology, Heart Rate Variability: Standards of measurement, physiological interpretation and clinical use, European Heart Journal, 17 (1996) 354-381.
66. N.V. Thakor, S. Tong, Advances in quantitative electroencephalogram analysis methods, Annual Reviews 6 (2004) 453-495.
67. P.D. Thompson, B.D. Levine, Protecting Athletes From Sudden Cardiac Death, JAMA, 296(13) (2006) 1648-1650.
68. M. P. Tulppo, T. H.Makikallio, T. E.Takala, T. Seppanen, H. V.Huikuri, Quantitative beat-to-beat analysis of heart rate dynamics during exercise, American Journal of Physiology- Heart and Circulatory Physiology, 271, (1996) H244-252.
69. R. Wariar, C. Eswaran, Integer coefficient bandpass filter for the simultaneous removal of baseline wander, 50 and 100 Hz interference from the ECG, Medical & Biological Engineering & Computing 29(3) (1991) 333-336.
70. C.L. Webber Jr and J.P. Zbilut, Dynamical assessment of physiological systems and states using recurrence plot strategies, Journal of Applied Physiology 76 (1994) 965-973.
71. M. A.Woo, W. G. Stevenson, D. K.Moser, R. B.Trelease, R. H.Harper, Patterns of beat-to-beat heart rate variability in advanced heart failure, American Heart Journal, 123, (1992) 704-707.
72. J.P. Zbilut , C.L Webber Jr, Embeddings and delays as derived from quantification of recurrence plots, Physics. Letters A 171 (1992) 199-203.

73. J.P. Zbilut, N. Thomasson , C. L. Webber, Recurrence quantification analysis as a tool for nonlinear exploration of nonstationary cardiac signals, Medical Engineering & Physics 24 (2002) 53–60
74. Z. Zhao , C. Ma, An intelligent system for noninvasive diagnosis of coronary artery disease with EMD-TEO and BP neural network, International Workshop on Education Technology and Training and International Workshop on Geoscience and Remote Sensing 2 (2008) 631-635.